Enantioselective Cathodic Reduction of 4-Methylcoumarin: Dependence of Selectivity on Reaction Conditions and Investigation of the Mechanism**

Merete Folmer Nielsen,* Belen Batanero, Thorsten Löhl, Hans J. Schäfer,* Ernst-Ulrich Würthwein, and Roland Fröhlich

Dedicated to Professor Dieter Seebach on the occasion of his 60th birthday

Abstract: The cathodic reduction of 4-methylcoumarin (**1**) in acidic methanol/water in the presence of yohimbine leads to formation of a mixture of the hydrogenation product 4-methyl-3,4-dihydrocoumarin (**2**), with an enantiomeric excess (*ee*) of (*R*)-**2** of 0–67%, and the hydrodimer **3**. The relative yields of **2** and **3** and the *ee* of **2** depend on a number of experimental parameters such as pH, supporting electrolyte, working potential, and the concentrations of substrate and yohimbine, as demonstrated by a series of preparative-scale experiments. In addition, a series of voltammetric and kinetic measurements were carried out to investigate the influence of the individual experimental parameters. Three mechanistic possibilities have been examined, and by combination of the analytical data with the results of the preparative experiments, a single model is put forward which is in accord with the available results. The main features of the mechanistic model can be summarized as follows: 1) under acidic conditions (pH 2–3) the electroactive species is a complex between **1** and H_3O^+, the reduction of which leads to an enolic radical; 2) this radical is not reduced at the working potential but tautomerizes into the more easily reduced keto radical or dimerizes; 3) the keto radical is reduced and further protonated; 4) the function of the yohimbineH^+ is to catalyze the tautomerization and enantioselectively protonate the final carbanion. Additionally, we conclude that the concentration of yohimbine in the immediate vicinity of the electrode is considerably higher than its stoichiometric concentration. Quantum chemical calculations demonstrate that *si* protonation of the intermediate anion by yohimbineH^+ to give (*R*)-**2** is energetically favored.

Keywords
enantioselective protonations · kinetics · quantum chemical calculations · reductions · voltammetry

Introduction

High stereoselectivity has been perfected in many chemical reactions.[1] For electrochemical conversions, the range of reactions, the attainable selectivities, and the level of mechanistic knowledge are far less advanced. Nevertheless, considerable progress has been made in the development of stereoselective electroorganic reactions in recent years,[2] and high diastereoselectivities have been achieved in both cathodic and anodic conversions. In cathodic hydrodimerization of cinnamic esters and amides with chiral alcohols[3] and oxazolidines[4] as auxiliaries, diastereoselectivities up to 95% *de* have been reached. Chiral phenylglyoxylic amides have been cathodically reduced to the corresponding mandelic acid derivatives with diastereoselectivities up to 92% *de*.[5] Auxiliary induced diastereoselectivities up to 86% *de* have been achieved in radical heterocoupling reactions of radicals generated by anodic decarboxylation.[6] High simple diastereoselectivities have been reported for cathodic[7] and anodic cyclizations.[8] Enantioselective conversions have been communicated for the cathodic hydrogenation of ketones with chiral supporting electrolytes as inductors.[9] Carbonyl compounds[10–12] and enones[13, 14] have been enantioselectively reduced with catalytic amounts of alkaloids. In an indirect electrolysis, *rac*-1-phenylethanol was kinetically resolved with TEMPO as mediator and sparteine as chiral inductor;[15] 2-naphthol has been coupled under similar conditions to give 1,1′-binaphthol with 99.5% *ee*,[16] and the enantioselective Sharpless bishydroxylation[17] has been performed as an indirect anodic oxidation.[18] Enantioselective electroenzymatic conversions are increasingly being developed.[19]

Enantioselective reduction of the prochiral enone 4-methylcoumarin (**1**) in methanol/buffer solution in the presence of

[*] Prof. Dr. H. J. Schäfer, Dr. B. Batanero, Dr. T. Löhl, Prof. Dr. E.-U. Würthwein, Dr. R. Fröhlich
Organisch-Chemisches Institut der Universität Münster
Corrensstrasse 40, D-48149 Münster (Germany)
Fax: Int. code + (251)83-39772
e-mail: schafeh@uni-muenster.de
Dr. M. F. Nielsen
Department of Chemistry, Symbion Science Park, University of Copenhagen
DK-2100 Copenhagen (Denmark)
Fax: Int. code + 3532-1810
e-mail: m.f.nielsen@symbion.ki.ku.dk

[**] Electroorganic Synthesis, Part 64. Part 63: K. Möller, H. J. Schäfer, *Electrochim. Acta* **1997**, *42*, 1971–1978.

  0947-6539/97/0312-2011 $ 17.50+.50/0

alkaloids such as sparteine, yohimbine or narcotine as chiral catalysts has been reported by Grimshaw et al. to give chiral 4-methyl-3,4-dihydrocoumarin (**2**) and optically inactive hydrodimer **3** (Scheme 1).[13] The highest induction was found for

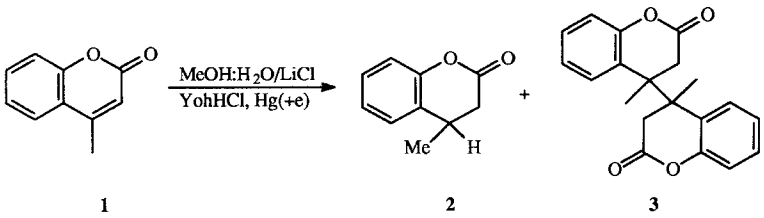

1 **2** **3**

Scheme 1. Cathodic reduction of 4-methylcoumarin (**1**).

sparteine (17% *ee*), but the chemical yield of **2** was low (4%), and the hydrodimer **3** was the main product (89%). By carrying out the electrolysis at lower pH and using yohimbine as catalyst, the optical yield was increased to 47% *ee* but the chemical yield of **2** (18%) remained moderate.[14a]

The aim of the present study was a) to increase the chemical yield and enantiomeric excess of **2** and b) to gain insight into the reaction mechanism. The effect of reaction conditions on the chemical yield and enantioselectivity of **2** was investigated by preparative-scale electrolyses. The kinetics and mechanism of the reduction of **1** under different experimental conditions were studied by application of electroanalytical measurements in an attempt to rationalize the results of the preparative experiments on a mechanistic basis.

Abstract in German: *Die kathodische Reduktion von 4-Methylcumarin (**1**) in saurem, wäßrigem Methanol führt in Gegenwart von Yohimbin zu 4-Methyl-3,4-dihydrocumarin (**2**) mit einem Enantiomerenüberschuß (ee) von 0–67% für (R)-**2** und den Hydrodimeren rac- und meso-**3**. Die Ausbeuten von **2** und **3** und der Enantiomerenüberschuß von **2** hängen vom pH-Wert, dem Elektrolyten, dem Kathodenpotential und den Konzentrationen von **1** und Yohimbin ab. Zusätzlich wurde voltammetrisch der Einfluß der experimentellen Reaktionsgrößen untersucht. Drei verschiedene mechanistische Möglichkeiten wurden geprüft, und aus der Kombination der analytischen Daten mit den Ergebnissen der präparativen Experimente wurde folgender Reaktionsweg vorgeschlagen: Unter sauren Bedingungen (pH 2–3) ist die elektroaktive Spezies ein Komplex aus **1** und H_3O^+, dessen Reduktion zur Bildung eines enolischen Radikals führt. Dieses Radikal wird beim Arbeitspotential nicht reduziert, sondern dimerisiert oder tautomerisiert in das leichter reduzierbare Ketoradikal. Das Ketoradikal wird reduziert und anschließend protoniert. Die Wirkung des protonierten Yohimbin besteht darin, die Tautomerisierung zu katalysieren und das Carbanion abschließend enantioselektiv zu protonieren. Aus den Ergebnissen wird weiterhin gefolgert, daß die Yohimbin-Konzentration nahe der Elektrode gegenüber der Konzentration in Lösung beträchtlich erhöht ist. Quantenchemische Rechnungen zeigen, daß die si Protonierung des intermediären Anions durch protoniertes Yohimbin, die zu (R)-**2** führt, energetisch begünstigt ist.*

Results and Discussion

Preparative Electrolyses: It has previously been shown that in the enantioselective reduction of **1** to **2** at pH 2–3, yohimbine (**4**) induced a higher enantiomeric excess than other alkaloids;[14a] **4** was therefore the only alkaloid used in this study. Since the preparative results of this (see below) and of previous studies[13, 14] indicate that several experimental parameters influence the product distribution and the *ee* of **2**, the approach in the mechanistic studies has been to investigate the effect of the parameters solvent, supporting electrolyte, medium acidity and the presence of yohimbine individually, in an attempt to analyze the individual effects of the parameters on the mechanism.

In preparative electrolyses, 4-methylcoumarin was electrolyzed at different acidities, cathode potentials, and concentrations of **1** and yohimbine (**4**) in a divided beaker or flow cell. 4-Methyl-3,4-dihydrocoumarin (**2**), the hydrodimer 4,4′-dimethyl-4,4′-bis-3,4-dihydrocoumarin (**3**), 3-(2′-hydroxyphenyl)butanoic acid (**5**) and methyl 3-(2′-hydroxyphenyl)-butanoate (**6**) were obtained as products. The last two compounds arise from hydrolysis and methanolysis of **2**; they were relactonized into **2** by heating the crude product with *p*-toluenesulfonic acid in toluene. The configuration of the excess enantiomer of (*R*)-**2** was assigned according to ref. [13e], the enantiomeric excess of (*R*)-**2** was determined by GLC. The two diastereomers of **3** could be separated by HPLC. The configuration of the higher melting diastereomer was assigned by X-ray crystallography to be the *rac* form.[20] In general *rac*-**3** was obtained in excess and optically inactive. The yields of recovered **1** and of the products **2** and **3** were determined by calibrated GLC. The dependence of the chemical yields of **2** and **3** and the enantioselectivity of **2** on different experimental parameters is summarized in Tables 1–6.

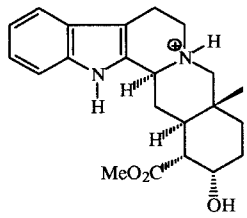

4-H+

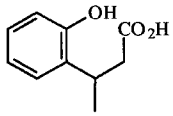

5

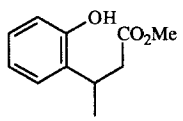

6

The data in Table 1 show that an increase of the LiCl concentration increases both the *ee* and the chemical yield of **2**, and the data in Table 2 indicate that the presence of Li^+ is essential for

Table 1. Dependence of the chemical yield of **2** and **3** and the *ee* of **2** on the LiCl concentration.[a]

[b]	*E* (V) vs. SCE	pH	[YohH$^+$] (mM)	[LiCl] (M)	**2** Yield (%)	**3** Yield (%)	**1** Yield (%)	**2** *ee* (%)
3	−1.5	2	2	1.5	51	9	26	58
9	−1.5	2	2	0.5	30	5	45	48

[a] Conditions: flow cell: 10 mL of a 0.13 M solution of **1** in MeOH/H_2O (1:1) were added over 6 h to 650 mL electrolyte; working electrode: Hg; solvent: MeOH/H_2O (1:1). [b] Experiment number.

0947-6539/97/0312-2012 $ 17.50+.50/0 *Chem. Eur. J.* **1997**, *3*, No. 12

Table 2. Dependence of the chemical yield of **2** and **3** and the *ee* of **2** on the nature of the supporting electrolyte.[a]

[b]	*E* (V) vs. SCE	pH	[LiCl] (M)	[Bu_4NBr] (M)	**2** Yield (%)	**3** Yield (%)	**1** Yield (%)	**2** *ee* (%)
12	−1.5	2	1.5	–	32	16	20	60
13	−1.5	2	–	0.5	5	64	9	5

[a] Conditions: beaker cell: 6 mL of a 0.16 M solution of **1** in MeOH/H_2O (1:1) were added during 3 h to 200 mL electrolyte; 2 mM yohimbine hydrochloride; working electrode: Hg; solvent: MeOH/H_2O (1:1). [b] Experiment number.

achieving good enantioselectivity and a reasonable yield of **2**. With Bu_4NBr as supporting electrolyte, the formation of hydrodimer **3** is increased at the expense of **2**, and almost no optical induction is obtained for **2**.

One can summarize the effect of the reduction potential, pH and yohimbinium concentration (Table 3) as follows: the influence of the reduction potential and pH cannot be separated since increasing acidity shifts the reduction potential of **1** to anodic values. At pH 3 the conversion of **1** is higher at −1.6 than at −1.5 V, whilst at pH 2 a working potential of −1.5 V is sufficient to achieve a good conversion of **1**. At pH 2 a higher enantioselectivity of **2** is favored by a less negative reduction potential (−1.5 instead of −1.6 V). Increasing the acidity to pH 1.5 increases the yield of **2** and retains a high *ee*. However, the reaction is now difficult to control due to the competing hydrogen discharge; a further decrease in pH is not experimentally possible. Increasing the pH lowers the enantioselectivity. At pH 2 an increase of the yohimbinium concentration favors both the yield of **2** and the enantioselectivity. In an electrolysis at pH 7 and a reduction potential of −1.6 V in water/methanol (1/1) as solvent and a 2 mM concentration of yohimbine, 7% **2** with 9% *ee*, 65% **3**, and 27% **1** were obtained.

Mercury is essential as cathode material (Table 4) because of its high overpotential for hydrogen evolution. The reduction of **1** overlaps with the proton discharge, so each diminution of the hydrogen overpotential of the cathode, as in the case of glassy carbon or graphite, decreases the conversion of **1**; also the *ee* of **2** decreases sharply. In Expt. 3 (Table 5) a low concentration of **1** was maintained by continuous addition of **1** to the electrolyte in amounts proportional to its estimated rate of conversion. It can be estimated that for 75% of the electrolysis time the concentration of **1** in Expt. 3 is about 400 times smaller than in Expt. 11. As the results show, decreasing the concentration of **1** does not influence the enantiomeric excess, but lowers the yield of the hydrodimer **3**. An increase in the water content of the solvent increases the yield of **2** and the conversion of **1** (Table 6), while the yield of **3** decreases and there is no effect on the enantioselectivity.

Table 4. Dependence of the chemical yield of **2** and **3** and the *ee* of **2** on the cathode material.[a]

[b]	*E* (V) vs. SCE	pH	Electrode	[LiCl] (M)	MeOH:H_2O	**2** Yield (%)	**3** Yield (%)	**1** Yield (%)	**2** *ee* (%)
12	−1.5	2	Hg	1.5	1:1	32	16	20	60
14	−1.5	2	Graphite	1.5	1:1	5	3	90	5
15	−1.5	2	Glassy C	1.5	1:1	1	8	90	10

[a] Conditions as [a] in Table 2, except for the cathode material. [b] Experiment number.

Table 5. Dependence of the chemical yield of **2** and **3** and the *ee* of **2** on the concentration of **1**.[a]

[b]	*E* (V) vs. SCE	pH	Electrode	[LiCl] (M)	MeOH:H_2O	**2** Yield (%)	**3** Yield (%)	**1** Yield (%)	**2** *ee* (%)
3 [a]	−1.5	2	Hg	1.5	1:1	51	9	26	58
11 [c]	−1.5	2	Hg	1.5	1:1	50	25	17	55

[a] As [a] in Table 1; 10 ml of a 0.13 M solution of **1** in MeOH/H_2O (1:1) were added dropwise during 6 h to 650 mL electrolyte. [b] Experiment number. [c] A 1.5 mM solution of **1** in 1.5 M LiCl in MeOH/H_2O (1:1) was electrolyzed for 6 h.

Table 6. Dependence of the chemical yield of **2** and **3** and the *ee* of **2** on the solvent composition.[a]

[b]	*E* (V) vs. SCE	pH	[LiCl] (M)	MeOH:H_2O	**2** Yield (%)	**3** Yield (%)	**1** Yield (%)	**2** *ee* (%)
12	−1.5	2	1.5	1:1	32	16	20	60
16	−1.5	2	1.5	1:2	36	9	16	67
17	−1.5	2	1.5	1:4	43	6	7	65

[a] Conditions as [a] in Table 2. [b] Experiment number.

Additionally, **1** was electrolyzed in DMF (1.5 M LiCl) in the presence of 2.5 mM yohimbine hydrochloride at a cathode potential of −1.5 V vs. SCE. The acidity was controlled by the addition of trifluoroacetic acid and was kept at a nearly constant concentration of 1 mM; 14% racemic **2** and 65% **3** were obtained.[14c]

Electroanalytical Investigations: In a recent study of the electrochemical reduction of a series of cinnamic acid esters, it was found[3b, c] that the competition between dimerization and formation of the dihydro product was significantly different when the reduction was carried out in MeOH rather than in DMF. Not only the product distribution but also the reaction mechanism was found to be very different in the two solvents. Since **1** is structurally related to the cinnamates, the mechanistic studies

Table 3. Dependence of the chemical yield of **2** and **3** and the *ee* of **2** on the reduction potential, the yohimbine concentration and the pH.[a]

[b]	*E* (V) vs. SCE	pH	[$YohH^+$] (mM)	[LiCl] (M)	**2** Yield (%)	**3** Yield (%)	**1** Yield (%)	**2** *ee* (%)
1	−1.5	2	0.25	1.5	19	27	23	42
2	−1.6	2	0.25	1.5	32	52	3	21
3	−1.5	2	2	1.5	51	9	26	58
4	−1.6	2	2	1.5	44	33	13	35
5	−1.5	3	0.25	1.5	3	2	92	54
6	−1.6	3	0.25	1.5	33	25	30	38
7	−1.5	3	2	1.5	8	2	86	6
8	−1.6	3	2	1.5	9	15	67	14
10	−1.45	1.5	2	1.5	61	9	17	63

[a] Conditions as [a] in Table 1. [b] Experiment number.

in this work include characterization of the reduction of **1** in DMF, as well as in pure MeOH and in a MeOH/H_2O mixture.

Voltammetric Studies of 1 in DMF: Cyclic voltammetry of **1** in DMF shows a single reduction peak, which at low scan rates (below ca. 1 Vs^{-1}) is chemically irreversible. At higher scan rates the process becomes chemically reversible, and an $E^0(\mathbf{1})$ value of -1.813 V vs. SCE was determined. Comparison of the values of $i_p/(C^0(\mathbf{1})v^{1/2})$ obtained at low scan rates, where the process is chemically irreversible, and at high scan rates, where it is chemically reversible, shows that the number of electrons transferred is constant and equal to unity (i_p denotes the peak current, $C^0(\mathbf{1})$ the stoichiometric concentration of **1**, and v the scan rate).

The combined reaction order in **1** and $\mathbf{1}^{\bullet -}$ was determined by derivative cyclic voltammetry (DCV) by measuring $v_{0.5}$ as a function of $C^0(\mathbf{1})$ ($v_{0.5}$ is the scan rate necessary to obtain $R'_1 = -i'_p(\mathrm{ox})/i'_p(\mathrm{red}) = 0.5$, where $i'_p(\mathrm{ox})$ and $i'_p(\mathrm{red})$ are the peak heights for oxidation and reduction, respectively, of the derivative of the voltammogram[21]). In the applied concentration range (0.5–8 mM) the apparent reaction order decreases from a value close to two at low concentrations (0.5–1 mM) to a value close to unity at high concentrations (4–8 mM), as shown by the curved plot in Figure 1. When $C^0(\mathbf{1}) = 4$ mM, the reaction is under purely kinetic control at low scan rates, and a value of $dE_p/d\log v = -18.9$ mV/decade was determined (Figure 2) by

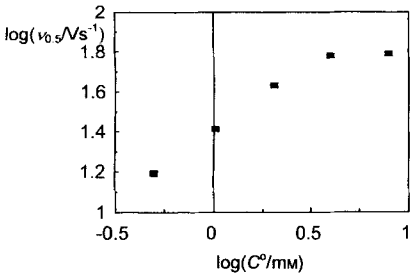

Figure 1. Dependence of the value of $v_{0.5}$ determined by DCV on the concentration of **1**. $C^0(\mathbf{1}) = 0.5$, 1, 2, 4 and 8 mM, in DMF (0.1 M Et_4NBr), $E^0 - E_{sw} = 0.2$ V, $T = 21$ °C, Hg/Pt electrode.

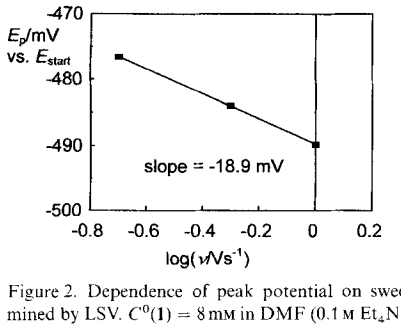

Figure 2. Dependence of peak potential on sweep rate, $v = 0.2$–1 Vs^{-1}, determined by LSV. $C^0(\mathbf{1}) = 8$ mM in DMF (0.1 M Et_4NBr), $T = 21$ °C, Hg/Pt electrode.

linear sweep voltammetry (LSV). The value of the half peak width $E_{p/2} - E_p$ was 43.7 mV. These observations are in fair agreement with a mechanism involving an electrochemically reversible electron transfer followed by rate-determining dimerization of two radical anions [Eqs. (1) and (2) in Scheme 2]. This mechanism is theoretically predicted[22] to give $E_{p/2} - E_p = 38.8$ mV and $dE_p/d\log v = -19.4$ mV/decade under purely kinetic conditions.

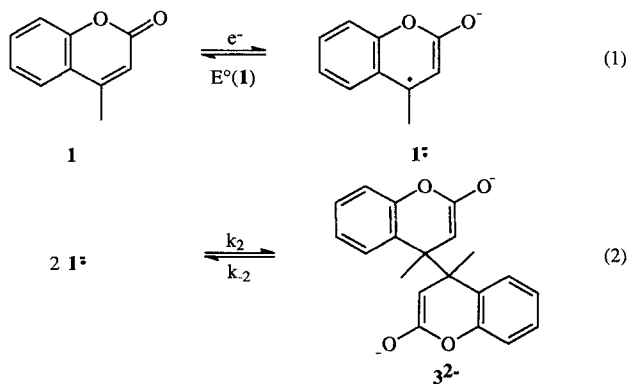

(1)

(2)

(3)

Scheme 2. Mechanism of the cathodic hydrodimerization of **1** to **3** in DMF.

The dianion formed by dimerization is subsequently protonated by residual water in the DMF [Eq. (3) in Scheme 2], but since the rate of dimerization increases with increasing concentration of **1**, protonation may become rate-determining at high values of $C^0(\mathbf{1})$. Consequently, the dimerization process may be partially reversed during the anodic scan of the DCV experiment if the dimerization equilibrium is not displaced too far to the right, and this gives rise to higher values of $R'_1 = -i'_p(\mathrm{ox})/i'_p(\mathrm{red})$ than in the case of an irreversible dimerization. Experimentally this behavior gives rise to apparent reaction orders $1 + d\log v_{0.5}/d\log C^0(\mathbf{1})$ smaller than 2, explaining the curved plot in Figure 1. An approximate second-order rate constant k_2 for the dimerization step can be calculated from the value of $v_{0.5}$ at $C^0(\mathbf{1}) = 0.5$ mM and theroretical data (see Experimental Section), assuming that the rate-determining step at this concentration of **1** is dimerization of two radical anions. The value of $k_2 = 1.5 \times 10^5\ M^{-1}s^{-1}$ calculated in this way may be compared with the value of $k_2 = 1.8 \times 10^5\ M^{-1}s^{-1}$ determined from the values of $E_p - E^0$ obtained at $C^0(\mathbf{1}) = 8$ mM and $v = 0.2$, 0.5, and 1 Vs^{-1}, that is, under purely kinetic conditions, by Equation (i), which is valid for an irreversible dimerization of two radical anions.[22]

$$k_2 = \frac{3}{4}\left(\frac{Fv}{RTC^0(\mathbf{1})}\right)\exp\left[\frac{3F}{RT}(E_p - E^0) + 3 \times 0.902\right] \quad \text{(i)}$$

The two estimates of k_2 are identical within the precision of the measurements and may be compared with the value obtained for the dimerization of the radical anions derived from 4-cyanophenyl cinnamate ($k_2 = 5.7 \times 10^4\ M^{-1}s^{-1}$).[3b] The radical anion of this cinnamate has the largest dimerization rate constant in the series of ten alkyl and aryl cinnamates previously studied.[3b] The data for 4-cyanophenyl cinnamate showed exactly the same but less pronounced trend towards a shift in rate-determining step from dimerization to protonation with increasing concentration.

Voltammetric Studies of 1 in MeOH and in MeOH/H_2O (1/1): In MeOH (0.2 M Et_4NBr) **1** is also reduced in a one-electron process, but the chemical reaction following electron transfer is much faster than in DMF. The follow-up reaction may be partly outrun by using a scan rate of 1000 Vs^{-1} (which compares to a scan rate of about 10 Vs^{-1} in DMF) at a substrate concentra-

0947-6539/97/0312-2014 $ 17.50+.50/0 Chem. Eur. J. 1997, 3, No. 12

tion of 0.5 mM, which allows determination of $E^0(\mathbf{1a}) = -1.625$ V vs. SCE (Scheme 3). Thus the reduction takes place at a more anodic potential in MeOH than in DMF. The nature of the follow-up reaction was studied by DCV in the scan-rate range $v = 50-1000\ \mathrm{Vs^{-1}}$, and by LSV at low scan rates ($v = 0.2-10\ \mathrm{Vs^{-1}}$) where the reaction is under purely kinetic control. The values of $dE_p/d\log v = -19.5$ to -21.6 mV/decade and $dE_p/d\log C^0 = 17.8$ mV/decade obtained by LSV (Figures 3 and 4) indicate that the only reaction following electron transfer is dimerization of two radical anions.[22]

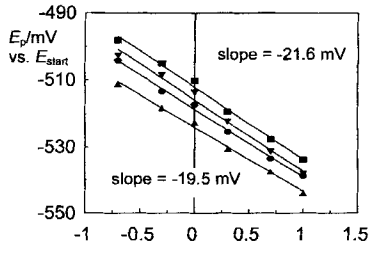

Figure 3. Dependence of peak potential on sweep rate, $v = 0.2-10\ \mathrm{Vs^{-1}}$, determined by LSV at $C^0(\mathbf{1}) = 1$ mM (▲), 2 mM (●), 4 mM (▼) and 8 mM (■) in MeOH (0.2 M Et_4NBr), $T = 21$ °C, Hg/Pt electrode. The values of $dE_p/d\log v$ increase systematically from $C^0(\mathbf{1}) = 1$ mM (−19.5 mV/decade) to $C^0(\mathbf{1}) = 1$ mM (−21.6 mV/decade).

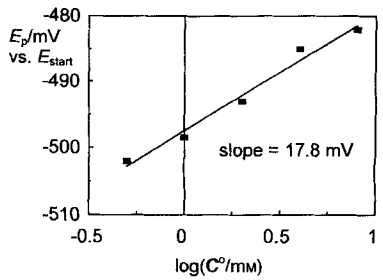

Figure 4. Dependence of peak potential on the concentration of **1**, $C^0(\mathbf{1}) = 0.5-8$ mM, determined by LSV at $v = 1\ \mathrm{Vs^{-1}}$ in MeOH (0.2 M Et_4NBr), $T = 21$ °C, Hg/Pt electrode.

This is further supported by the values of the half peak width $E_{p/2} - E_p$ measured in the LSV experiments (Table 7), which are in agreement with the theoretical value (38.7 mV[22]) for a simple dimerization mechanism. By application of Equation (i),[22] the second-order rate constant was determined, Table 7, giving an average of $k'_2 = 1.4 \times 10^7\ \mathrm{M^{-1}s^{-1}}$. In good agreement with this value, $k'_2 = 1.7 \times 10^7\ \mathrm{M^{-1}s^{-1}}$ was determined by fitting the DCV data to theoretical data (see Experimental Section) for the same mechanism (Figure 5). Comparison shows that the rate constant for dimerization is two orders of magnitude larger in MeOH than in DMF (see above).

Table 7. Peak shifts, $E_p - E^0$, peak shapes, $E_{p/2} - E_p$, and second-order rate constants for dimerization determined by LSV of **1** in MeOH (0.2 M Et_4NBr).[a]

$C^0(\mathbf{1})$ (mM)	$E_{p/2} - E_p$ (mV)	$E_p - E^0$ (V) [b]	k'_2 ($\mathrm{M^{-1}s^{-1}}$) [c]
0.5	40.7	0.0250	1.69×10^7
1.0	41.7	0.0285	1.28×10^7
2.0	40.1	0.0340	1.22×10^7
4.0	38.5	0.0420	1.57×10^7
8.0	36.8	0.0450	1.12×10^7
			$(1.4 \pm 0.2) \times 10^7$ [d]

[a] Hg/Pt electrode, $T = 22$ °C, $v = 1\ \mathrm{Vs^{-1}}$. [b] E^0 determined by CV at $v = 1000\ \mathrm{Vs^{-1}}$ as $^1/_2(E_p^{red} + E_p^{ox})$ at $C^0(\mathbf{1}) = 0.5$ mM. [c] Determined from $E_p - E^0$ and Equation (i). [d] Average of values above.

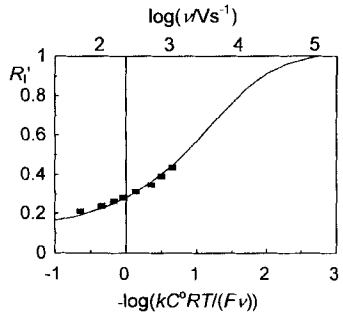

Figure 5. Fit of experimental values of R'_1 vs. log$v$ measured by DCV ($E^0 - E_{sw} = 0.2$ V) for **1**, $C^0(\mathbf{1}) = 0.5$ mM, in MeOH (0.2 M Et_4NBr) to theoretical data for the mechanism described in Scheme 3 with rate-determining dimerization. $T = 21$ °C, Hg/Pt electrode.

Analogous measurements were carried out in MeOH/H_2O (1/1) (0.2 M Et_4NBr), and the results (Table 8 and Figures 6–8) were qualitatively identical to those obtained in pure MeOH:

Table 8. Peak shifts, $E_p - E^0$, peak shapes, $E_{p/2} - E_p$, and second-order rate constants for dimerization determined by LSV of **1** in MeOH/H_2O (1:1) (0.2 M Et_4NBr).[a]

$C^0(\mathbf{1})$ (mM)	$E_{p/2} - E_p$ (mV)	$E_p - E^0$ (V) [b]	k'_2 ($\mathrm{M^{-1}s^{-1}}$) [c]
0.5	38.5	0.0223	1.26×10^7
0.9	38.7	0.0287	1.50×10^7
1.9	38.2	0.0352	1.53×10^7
4.0	38.5	0.0409	1.43×10^7
8.2	38.6	0.0448	1.11×10^7
			$(1.4 \pm 0.2) \times 10^7$

[a] Hg/Pt electrode, $T = 20$ °C, $v = 1\ \mathrm{Vs^{-1}}$. [b] E^0 determined by CV at $v = 1000\ \mathrm{Vs^{-1}}$ as $^1/_2(E_p^{red} + E_p^{ox})$ at $C^0(\mathbf{1}) = 0.5$ mM. [c] Determined from $E_p - E^0$ and Equation (i). [d] Average of values above.

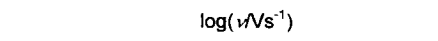

Figure 6. Dependence of peak potential on the sweep rate, $v = 0.2-10\ \mathrm{Vs^{-1}}$, determined by LSV at $C^0(\mathbf{1}) = 0.5$ mM (△), 1 mM (●), 2 mM (▼), 4 mM (■), and 8 mM (□) in MeOH/H_2O (1/1) (0.2 M Et_4NBr), $T = 21$ °C, Hg/Pt electrode. The values of $dE_p/d\log v$ are all in the range -18.8 to -21.0 mV/decade.

$E^0(\mathbf{1a}) = -1.635$ V vs. SCE, $k'_2 = 1.4 \times 10^7\ \mathrm{M^{-1}s^{-1}}$ by Equation (i), and $k'_2 = 2.7 \times 10^7\ \mathrm{M^{-1}s^{-1}}$ by fitting the DCV data to the working curve. The reason for the slightly larger discrepancy between the two types of measurements in this case was not further explored.

The most likely mechanism under hydroxylic conditions is outlined in Scheme 3. The introduction of a specifically solvated (by a hydrogen bond) radical anion, $\mathbf{1a}^{\bullet-}$, is in agreement with

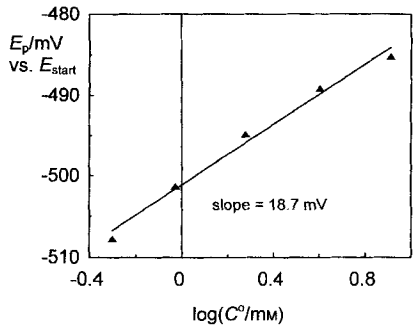

Figure 7. Dependence of peak potential on the concentration of **1**. $C^0(\mathbf{1}) = 0.5$–8 mM, determined by LSV at $v = 1\ Vs^{-1}$ in MeOH/H_2O (1/1) (0.2 M Et_4NBr), $T = 21\,^{\circ}C$. Hg/Pt electrode.

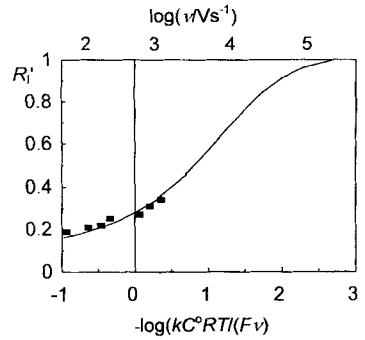

Figure 8. Fit of experimental values of R'_1 vs. log$v$ measured by DCV ($E^0 - E_{sw} = 0.2$ V) for **1**. $C^0(\mathbf{1}) = 0.5$ mM, in MeOH/H_2O (1/1) (0.2 M Et_4NBr) to theoretical data for the mechanism described in Scheme 3 with rate-determining dimerization. $T = 21\,^{\circ}C$, Hg/Pt electrode.

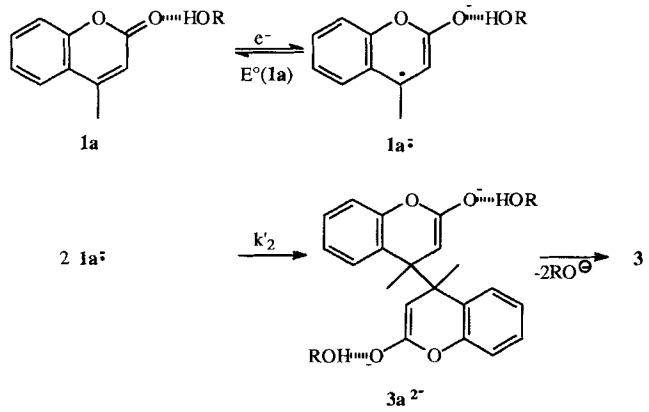

Scheme 3. Mechanism of the cathodic hydrodimerization of **1** to **3** in MeOH or MeOH/H_2O.

general views of anion solvation in hydroxylic media[23] and is also in good agreement with the fact that the dimerization process in DMF is considerably slower since it takes place between two nonspecifically solvated radical anions. This interpretation of the change in behavior when the solvent is changed from DMF to MeOH or MeOH/H_2O is analogous to the interpretation given previously[3c] for the similar changes observed for aryl cinnamates.

Voltammetric Studies of ***1*** *in MeOH and in MeOH/H_2O (1/1) under acidic conditions:* From the results obtained in the absence of added acids, it appears that the radical anion reacts exclusively by the dimerization pathway leading to the hydrodimer **3**. In order to obtain the dihydro product **2**, it is therefore necessary to add a strong proton donor to compete favorably with the fast dimerization process. To mimic the conditions of the preparative work HCl was used as the proton source.

The voltammogram obtained at $C^0(\text{HCl}):C^0(\mathbf{1}) = 1:2$ (Figure 9) gives a qualitative picture of the tremendous effect of strong acid on the reduction of **1**; the reduction peak splits into

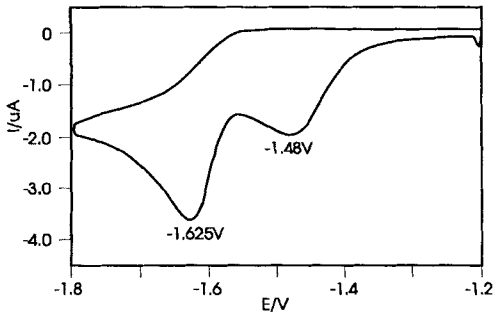

Figure 9. Cyclic voltammogram of **1** (2 mM) in MeOH/H_2O (1/1) (0.5 M LiCl) in the presence of 1 mM HCl. $v = 1\ Vs^{-1}$.

two peaks due to the complete consumption of the protons before all the substrate is reduced. The more cathodic peak corresponds to the original reduction peak observed in the absence of acid, while the new, more anodic peak represents the reduction of a new species. The large difference in potential between the two peaks (>150 mV) is not compatible with a simple kinetic shift of part of the original peak, as can be observed in some cases when the substrate is stoichiometrically in excess with respect to an added reactant.[24] Assuming that a fast protonation of the radical anion leads to a normal $2e^-$, $2H^+$ process that can be described by a simple DISP1 mechanism with rate-determining proton transfer, the maximum kinetic shift will be less than 80 mV at $v = 1\ Vs^{-1}$ when $C^0(H^+) = 1$ mM.[24b]

When the concentration of acid is increased, the original peak disappears while the new reduction peak grows, and when the reaction is under pseudo-first-order conditions with respect to the concentration of protons [C^0(HCl): $C^0(\mathbf{1}) > 10$],[25] the voltammogram is severely distorted owing to the discharge of protons, which turns the new reduction peak into a shoulder on the broad proton reduction wave (Figure 10a). However, by use of scan rates above $10\ Vs^{-1}$, which makes the proton reduction cathodic, and by application of the first derivative which turns the potential of the "shoulder" into a local minimum (Figure 10b), it is possible to ob-

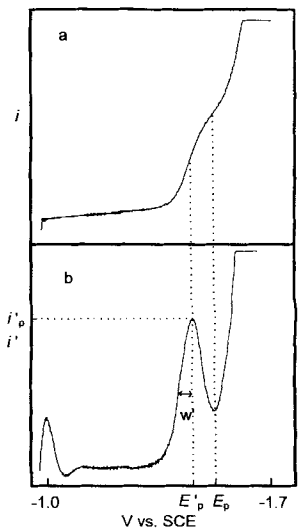

Figure 10. The current (a) and the first derivative (b) of the current for a linear potential sweep in the range −1.0 to −1.7 V vs. SCE at v = 100 Vs^{-1} on a 1 mM solution of **1** in MeOH/H_2O (1/1) (0.2 M Et_4NBr) upon addition of 10 mM HCl. $T = 21\,^{\circ}C$, Hg/Pt electrode.

0947-6539/97/0312-2016 $ 17.50+.50/0 Chem. Eur. J. 1997, 3, No. 12

tain information regarding the number of electrons and the change in potential with scan rate. Since the potential E'_p and height i'_p of the peak in the derivative signal is less affected by increasing proton concentration than the minimum, these parameters were chosen for the measurements. However, increasing proton concentration still broadened the derivative peak considerably, and it was therefore chosen to use $i'_p w'/v^{1/2}$ (where w' is the half peak width of the derivative peak; see Figure 10b) instead of $i'_p/v^{1/2}$ as the measure of the number of electrons transferred. The most important observations are: a) The reaction is a one-electron reaction as judged by comparing the normalized current $i'_p w'/v^{1/2}$ with the same quantity measured on the derivative peak of the "original" voltammogram obtained before addition of protons (Figure 11); the increase in $i'_p w'/v^{1/2}$ at the lowest scan rates is due to the contribution from proton discharge. b) The value of $dE'_p/d\log v$ is in the range -17.6 to -22.1 mV/decade (Figure 12). These observations indicate that the process has not changed into a $2e^-, 2H^+$ reduction upon addition of acid; instead the one-electron transfer is followed by a second-order reaction of the electrochemically formed species. Reliable measurements of $dE'_p/d\log C^0(HCl)$ were not possible since the shape of the background (the proton reduction) changed significantly with $C^0(HCl)$; however, the values of $dE'_p/d\log C^0(HCl)$ measured at the scan rates 100 and 200 $V s^{-1}$, for which the influence of the proton reduction on the substrate reduction is smallest, are in the range 51–56 mV/decade (Figure 13).

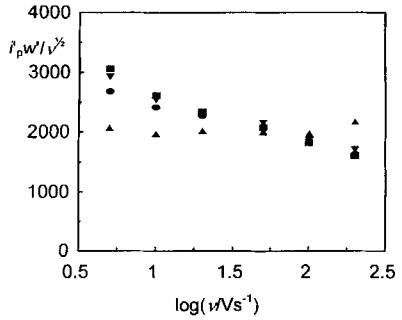

Figure 11. Normalized current, $i'_p w'/v^{1/2}$ (i'_p and w' are defined in Figure 10b) of the derivative signal at different concentrations of HCl, $C^0(HCl) = 0$ mM (▲), 10 mM (●), 20 mM (▼) and 40 mM (■) measured at different scan rates in the range $v = 5$–200 Vs^{-1} by LSV on the first derivative of the current. $C^0(\mathbf{1}) = 1$ mM in MeOH/H_2O (1:1) (0.2 M Et_4NBr), $T = 21$ °C, Hg/Pt electrode.

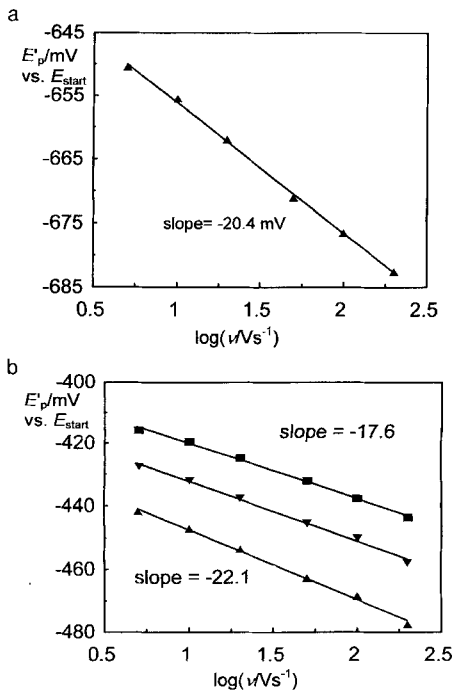

Figure 12. Peak potential dependence of the first derivative of the signal on the sweep rate at different concentrations of HCl measured by LSV. $C^0(\mathbf{1}) = 1$ mM in MeOH/H_2O (1/1) (0.2 M Et_4NBr), $T = 21$ °C, Hg/Pt electrode. a) $C^0(HCl) = 0$ mM; b); $C^0(HCl) = 10$ mM (▲), 20 mM (▼), and 40 mM (■).

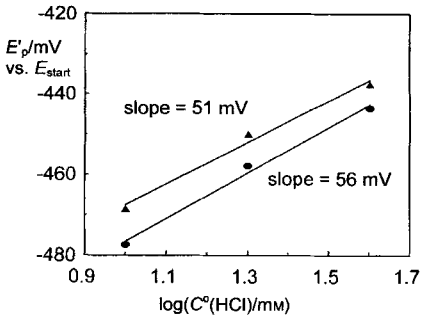

Figure 13. Peak potential dependence of the first derivative of the signal on the concentration of HCl, $C^0(HCl) = 10$, 20 and 40 mM, at two scan rates, $v = 100$ (▲) and 200 Vs^{-1} (●), determined by LSV. $C^0(\mathbf{1}) = 1$ mM in MeOH/H_2O (1/1) (0.2 M Et_4NBr), $T = 21$ °C, Hg/Pt electrode.

These observations can be interpreted by Scheme 4. The tight complex **1b** between the substrate and H_3O^+ is formed in a pre-equilibrium. Owing to the positive charge, this complex is expected to have a much more anodic value $E^0(\mathbf{1b})$ than the loosely hydrogen-bonded 4-methylcoumarin $E^0(\mathbf{1a})$ found under neutral conditions.

Although the equilibrium constant for formation of the complex probably is rather small (no new species can be detected by UV measurements in the presence of HCl), the rate constants for formation and dissociation of the complex are expected to be

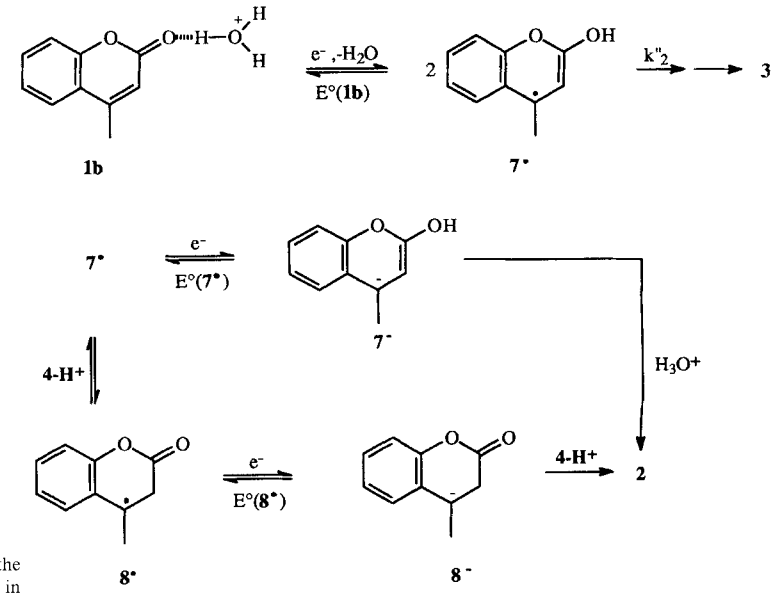

Scheme 4. Mechanism of the cathodic reduction of **1** to **2** and **3** in acidic MeOH/H_2O.

  0947-6539/97/0312-2017 $ 17.50+.50/0

high, that is, equilibrium is maintained during the voltammetric experiment even at scan rates up to 200 Vs^{-1}. Since the equilibrium in which the complex is formed will be displaced towards the complex with increasing concentration of HCl, the peak potential for the reduction of the complex is expected to shift in the positive direction by 60 mV with a tenfold increase in HCl concentration if the equilibrium constant for formation of the complex is small.[26]

Simultaneously with the electron transfer (or in an extremely fast and far-displaced equilibrium), the proton shifts from water to the keto group to give the oxygen-protonated radical anion **7'**. This neutral radical can then dimerize or be reduced, but it will be more difficult to reduce than the initial complex $[E^0(\mathbf{1b}) > E^0(\mathbf{7'})]$, in accordance with the one-electron height of the normalized derivative peak current. The corresponding reduction peak at a more cathodic potential will therefore overlap with the proton reduction process. Similar observations (i.e., that the neutral radical corresponding to an oxygen-protonated radical anion is more difficult to reduce than the substrate) have previously been made for alkyl cinnamates which are protonated by MeOH in MeOH,[3c] for benzaldehyde in aqueous buffers,[27] and for fuchsone and analogues in DMF in the presence of phenols.[28] In these cases, the radical formed by protonation of the radical anion is more difficult to reduce than the neutral hydrogen-bonded substrate; here this would correspond to $E^0(\mathbf{1b}) \gg E^0(\mathbf{1a}) > E^0(\mathbf{7'})$.

The rate constant for dimerization k_2'' of the two neutral radicals **7'** thus formed (Scheme 4) is expected to be larger than the rate constant k_2' for dimerization of the two specifically solvated radical anions formed in the absence of proton donors (Scheme 3),that is, $k_2'' > 10^7\ M^{-1}s^{-1}$ is expected. A fast dimerization as the dominant reaction following electron and proton transfer is in good agreement with the observed $dE_p''/d\log v \approx -20$ mV/decade, which indicates a second-order reaction of the product of the electrode process (under these conditions, the neutral radical **7'**).

The Effect of Li^+: The main effect of the addition of Li^+ (1.0 M) to a 1 mM solution of **1** in $MeOH/H_2O$ (1/1) (0.1 M Et_4NBr) is an anodic shift of the background (proton reduction) due to acidification of the medium by specific solvation of Li^+ by ROH. As a result the peak potential for reduction of **1** becomes slightly more anodic (5–15 mV), and the normalized peak height increases by about 30%. At the same time, the peak width increases from around 40 mV to around 50 mV, and the voltammograms become less reproducible.

Reduction of a 1 mM solution of **1** in the presence of Li^+ and 20 mM HCl also leads to broader derivative peaks than in the absence of Li^+, with a significant contribution to the height of the derivative peak from proton reduction. However, a value of $dE_p'/d\log v \approx -20$ mV/decade is also found in this case, and this indicates that the follow-up reaction is unchanged by the presence of Li^+.

The Effect of YohimbineH$^+$: Initially, the voltammetry of yohimbine hydrochloride (1 mM) was studied in $MeOH/H_2O$ (1:1) (0.1 M Et_4NBr) in the absence of **1**. A broad reduction peak ($E_{p/2} - E_p \approx 90$ mV) was found, 50–100 mV more cathodic (depending on the scan rate) than the peak corresponding to the reduction of **1** in neutral $MeOH/H_2O$ (1/1). This reaction is interpreted as a yohimbine-catalyzed reduction of protons, and this is confirmed by a large increase in the current upon addition of HCl (10 mM) to the solution without any significant change in peak potential. At low scan rates ($< 10\ Vs^{-1}$) the yohimbine-catalyzed reduction of protons is accompanied by adsorption, as shown in Figure 14. If Li^+ is added to the solution, the adsorption behavior also dominates at higher scan rates. Addition of yohimbineH$^+$ to a solution of **1** leads to a very broad and ill-defined voltammetric peak (Figure 15), especially when HCl and Li^+ also are present, which cannot be analyzed with confidence.

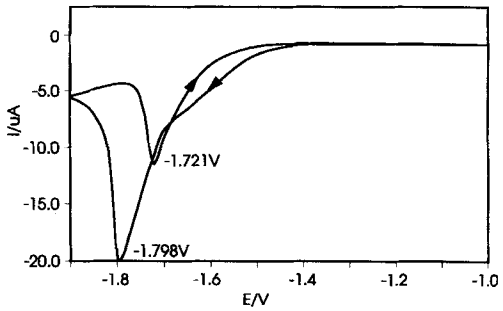

Figure 14. Cyclic voltammogram of yohimbine (2 mM) in the presence of 1 mM HCl in $MeOH/H_2O$ (1/1) (0.5 M LiCl), $v = 0.7\ Vs^{-1}$.

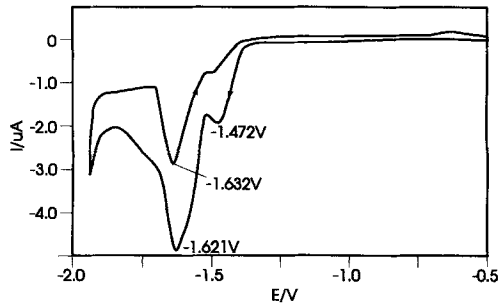

Figure 15. Cylic voltammogram of **1** (2 mM) in the presence of yohimbine and 1 mM HCl in $MeOH/H_2O$ (1/1) (0.5 M LiCl), $v = 1\ Vs^{-1}$.

From the voltammetry of yohimbineH$^+$ alone (in $MeOH/H_2O$ with Et_4NBr or LiCl as supporting electrolyte) it seems reasonable to suggest that it is the neutral yohimbine formed by reduction of the protons which is adsorbed. The reason is probably the much smaller solvation energy expected in hydroxylic media for the neutral form than for the protonated form, hence neutral yohimbine is almost insoluble.

From the analysis of the experiments carried out in the absence and presence of yohimbineH$^+$, there is no indication that the reduction of **1** in acidic $MeOH/H_2O$ with LiCl as supporting electrolyte in the presence of yohimbineH$^+$ should follow another reaction pathway than in the absence of yohimbineH$^+$ until the last step(s) which determine the fate of **7'**.

Mechanistic Proposals

The ill-behaved nature of voltammetry under experimental conditions analogous to the preparative ones means that the conclusions drawn about mechanistic features under these conditions

0947-6539/97/0312-2018 $ 17.50+.50/0 Chem. Eur. J. 1997, 3, No. 12

are necessarily somewhat speculative. However, from the combination of preparative results and mechanistic studies carried out in the absence of yohimbine, a number of conclusions can be drawn. In the absence of yohimbine, hydrogen evolution takes place at a more anodic potential than in its presence, and there is no enantiomeric excess in the formed **2**. Even small amounts of yohimbine (0.25 mM) give rise to significant *ee*'s in **2** (see Table 3). This points to an enhanced concentration of yohimbineH$^+$ at the electrode surface, and one possibility is that yohimbineH$^+$ is specifically incorporated (as a cation) into the double layer owing to a favorable interaction of the lipophilic alkaloid cation with the Hg electrode compared to its interaction with the highly hydrophilic bulk solvent. This view is supported by the fact that if the cation of the supporting electrolyte is changed from Li^+ to Bu_4N^+ there is a dramatic decrease in the *ee* of **2** (Table 2), which may be explained by an efficient competition for preferential incorporation of this nonacidic and lipophilic cation into the double layer due to the much larger concentration of Bu_4N^+ than of yohimibineH$^+$ (0.5 vs. 0.002 M) in the catholyte. Furthermore, the increase in the yield of **2** upon increasing the water content of the catholyte (Table 6) is consistent with enhanced incorporation of the yohimbineH$^+$ with increasing hydrophilicity of the solvent. Previous experiments[14a] have shown that increasing the stoichiometric concentration of yohimbine only leads to higher *ee* of **2** within a narrow concentration range. When the MeOH/H_2O ratio is 4/6, as in the previous study,[14a] the maximum effect of yohimbine is reached at a concentration of 0.25 mM. When MeOH/H_2O is 1/1, as in most of this study, the saturation effect is reached at a higher stoichiometric concentration according to the data in Table 3, which show that the *ee* of **2** at pH 2 (and independent of the working potential) is higher when 2 mM rather than 0.25 mM yohimbine is used. A specific interaction between yohimbineH$^+$ and mercury can not be ruled out, since a change in cathode material (Table 4) not only leads to a decrease in the chemical conversion of **1** due to increased hydrogen evolution but also to a much smaller *ee* of **2**.

The main mechanistic question is the exact function of yohimbineH$^+$ in the last steps of the reduction of **1**. Three possibilities will be discussed: 1) The neutral radical **7**$^\bullet$ is reduced to **7**$^-$, which is enantioselectively protonated by yohimbineH$^+$ in the last step. 2) YohimbineH$^+$ catalyzes the isomerization of **7**$^\bullet$ to the more easily reduced keto form **8**$^\bullet$, which is then reduced and enantioselectively protonated by yohimbineH$^+$. 3) Parallel to the reduction of **1b** to **7**$^\bullet$, yohimbineH$^+$ is reduced to a yohimbine–H$^\bullet$ complex, which enantioselectively transfers H$^\bullet$ to the radical **7**$^\bullet$.

The kinetic results obtained in neutral MeOH/H_2O clearly show that the medium is too weak an acid to protonate the radical anion, and this will still be the case in the presence of 2 mM yohimbineH$^+$ [pK_a (yohimbineH$^+$) = 7.1[29]]. The hydrogen-bonded radical anion **1a**$^{\bullet -}$ therefore mostly dimerizes, even at the low concentrations found during preparative electrolysis in MeOH/H_2O (65% **3**, 7% **2**), since **1a**$^{\bullet -}$ is not further reduced at the working potential of −1.6 V vs. SCE, which is close to the values of E^0(**1a**). When the medium is acidified with HCl, the mechanistic results show that it is the complex **1b** which is reduced, and this reduction takes place at a more anodic potential. At pH 3 the thermodynamic shift of the reduction potential is not sufficiently large for the reduction to be efficient at −1.5 V, as indicated by the low conversion of **1** in Table 3, whereas at pH 2 the thermodynamic shift is sufficiently large for **1** to be reduced at a working potential of −1.5 V. This is in excellent agreement with the potential of the peak of the derivative signal (ca. −1.40 V) determined by measurements in the presence of 10 mM HCl but in the absence of yohimbine.

Since the reduction of **1b** leads immediately to the neutral radical **7**$^\bullet$ (Scheme 4), a very important parameter is the reduction potential of **7**$^\bullet$. As mentioned above, it appears to be general that neutral radicals formed by protonation of radical anions at the oxygen atom are more difficult to reduce than the substrates from which they are derived.[3c, 27, 28] From measurements on the structurally related alkyl cinnamates in MeOH, the peak potential for reduction of the oxygen-protonated radical anion was found to be approximately 50–100 mV more cathodic than the value of E^0 for the substrate.[3c] Assuming a similar separation of the two reduction potentials for **1**, the peak potential for reduction of the oxygen-protonated radical anion E_p(**7**$^\bullet$) is expected to assume a value on the cathodic side of −1.7 V vs. SCE, and the mechanistic studies showed that addition of Li^+ did not shift the reduction of **7**$^\bullet$ to the potential of reduction of **1** at pH 2, or even in neutral solution. The first mechanistic possibility—the neutral radical **7**$^\bullet$ is reduced at the electrode to **7**$^-$, which is protonated by yohimbineH$^+$ to the enol tautomer of **2**—is therefore unlikely, since the electrolysis in all cases was carried out in the potential range −1.45 to −1.60 V vs. SCE, where heterogenous reduction of the intermediate **7**$^\bullet$ is unlikely to take place. Another argument against the direct heterogeneous reduction of **7**$^\bullet$ is that competing formation of dimer, which requires competition between further reduction and diffusion away from the electrode, is not lowered when the reduction is carried out at −1.6 V instead of at −1.5 V (Table 3).

The second mechanistic possibility, in which yohimbineH$^+$ catalyzes the isomerization of **7**$^\bullet$ to the more easily reduced keto form **8**$^\bullet$, which is then reduced and enantioselectively protonated by yohimbineH$^+$, may initially seem rather speculative. Quantum chemical calculations with MOPAC 6 lead to the following heats of formation: **7**$^\bullet$ −29.09 kcal mol^{-1}, **7**$^-$ −58.99 kcal mol^{-1}, **8**$^\bullet$ −32.86 kcal mol^{-1}, and **8**$^-$ −76.99 kcal mol^{-1}. These values indicate that the isomerization **7**$^\bullet \rightleftharpoons$ **8**$^\bullet$ is slightly exothermic (ΔE = −3.77 kcal mol^{-1}), and furthermore that the reduction of **8**$^\bullet$ to **8**$^-$ (ΔE = −44.13 kcal mol^{-1}) is much more exothermic than the reduction of **7**$^\bullet$ to **7**$^-$ (ΔE = −29.9 kcal mol^{-1}). In contrast to the enol radical **7**$^\bullet$ the keto radical **8**$^\bullet$ is expected to be more easily reduced than **1**, E^0(**1a**), in accordance with other systems in which the radical anion is protonated at a carbon atom, and for which the reaction changes from a 1F to a 2F process when proton donors are added.[30] A precise value of the reduction potential for **8**$^\bullet$ can not be obtained, but a value 200–400 mV more anodic than the value of E^0(**1a**), that is between −1.25 and −1.45 V, is likely, judged from the approximate relative values for other system[24c, 28]. The idea that yohimbineH$^+$ catalyzes the tautomerization of **7**$^\bullet$ to **8**$^\bullet$ is supported by a parallel study of the enantioselective hydrogenation of 3-methylinden-1-one[31] in which there is evidence for a change from a one- to a two-electron process in the presence of an alkaloid in acidic media.

A value of $E_p(\mathbf{8}^{\bullet})$ in the range -1.25 to -1.45 V shows that $\mathbf{8}^{\bullet}$ will be reducible at the working potentials used in the preparative experiments. Its reduction leads to formation of a strongly basic carbanion $\mathbf{8}^-$, which has to be protonated by yohimbineH$^+$ for the observed enantioselectivity. As discussed above, it is likely that the concentration of yohimbineH$^+$ is higher at the electrode surface than in the bulk when Li^+ is the supporting electrolyte cation, since even small amounts of yohimbineH$^+$ lead to a considerable *ee* in **2** (Table 3). The protonation therefore must take place very close to the surface, since if the weak acid yohimbineH$^+$ competed with the more abundant H_3O^+ (at pH 2) in the bulk, a much smaller *ee* of **2** would be expected. Catalysis of the isomerization by yohimbineH$^+$ must also take place close to the surface (in competition with diffusion of $\mathbf{7}^{\bullet}$ into the solution and dimerization), in good agreement with the observation that a much smaller yield of **2** relative to **3** is obtained when Bu_4N^+ is the supporting electrolyte cation, since Bu_4N^+ may compete favorably with yohimbineH$^+$ for incorporation into the double layer.

When the electrolysis is carried out at -1.6 V, simultaneous proton discharge becomes significant. Assuming that the proton discharge takes place via reduction of yohimbineH$^+$ to yohimbineH$^{\bullet}$, this parallel reduction will lower the concentration of yohimbineH$^+$ more at -1.6 V than at -1.5 V and thereby decrease the amount available for isomerization of $\mathbf{7}^{\bullet}$ to $\mathbf{8}^{\bullet}$ and for the enantioselective protonation of $\mathbf{8}^-$. This may explain the decreased *ee* in **2** at pH 2 when the electrolysis is carried out at -1.6 V instead of at -1.5 V (Table 3).

The competition between isomerization and dimerization of $\mathbf{7}^{\bullet}$ (and possibly dimerization of $\mathbf{8}^{\bullet}$) will obviously be influenced by the concentration of $\mathbf{7}^{\bullet}$, which, under otherwise identical conditions, is proportional to the concentration of **1**. The competing dimerization of the intermediate leading to the hydrodimer **3** will be favored by an increase in the substrate concentration (Table 5). A very low (0.1–0.2 mM) concentration of **1**, as is obtained by using a flow cell for the preparative electrolysis, is an advantage compared to previously published results for a beaker-type cell in which the total amount of **1** was added to the catholyte before electrolysis was initiated.[14a]

None of the preparative or mechanistic results are in disagreement with this second mechanistic possibility, outlined in Scheme 4, but a third mechanistic possibility has to be examined as well: that parallel to the reduction of **1b** to $\mathbf{7}^{\bullet}$, yohimbineH$^+$ is reduced to a yohimbine–H$^{\bullet}$ complex which enantioselectively transfers a hydrogen atom to the radical $\mathbf{7}^{\bullet}$. Regardless of whether the working potential for the preparative electrolysis is -1.5 or -1.6 V, the reduction of **1** is accompanied by proton reduction, which leads to evolution of hydrogen. Since yohimbine appears to be involved in the proton reduction and is abundant in the vicinity of the electrode (see above), one may envisage the proton reduction as a reduction of yohimbineH$^+$ to a yohimbine–H$^{\bullet}$ complex, which could act as an enantioselective H$^{\bullet}$ donor towards the radical $\mathbf{7}^{\bullet}$. This radical–radical combination is expected to be fast and could therefore compete with the fast dimerization of $\mathbf{7}^{\bullet}$ due to a higher concentration of yohimbine-H$^{\bullet}$ than of $\mathbf{7}^{\bullet}$. However, since the proton reduction is more efficient at -1.6 V than at -1.5 V the *ee* of **2** would be expected to be larger at -1.6 V than at -1.5 V (at pH 2), but the opposite is found (see Table 3). This third mechanistic possibility therefore seems to be less likely than the second, especially given that the overall similar behavior of the related system 3-methylinden-1-one is incompatible with this third mechanism, since the reduction process in that case takes place at a much more anodic potential.[31]

Quantum Chemical Modeling of the Enantioselective Proton Transfer from the Yohimbinium Cation (4-H$^+$) to the 4-Methyl-3,4-dihydrocoumarin Anion ($\mathbf{8}^-$): A last question concerns the possibility of explaining the preferred formation of (*R*)-**2** in the final proton transfer step. By using force-field methods and choosing a distinct distance between the proton in **4**-H$^+$ and C4 in $\mathbf{7}^-$ it has been calculated that the probability of *si* attack of **4**-H$^+$ at C4 in $\mathbf{7}^-$ leading to (*R*)-**2** is higher than that of *re* protonation leading to (*S*)-**2**.[14b] To make this statement more general and to transfer this model to substrates other than 4-methylcoumarin (**1**), it was desirable to calculate the different energies of the two diastereomorphic transition states for the *re* and *si* protonation of $\mathbf{8}^-$. For the calculation of these ion pairs, which contain 38 heavy atoms, the semiempirical method AM1[32] was used.

At first the simple model system **9**, the protonation of 4-methyl-4-*H*-pyranyl anion by ammonium cation, was investigated. The generally assumed,[33] preferred linear geometry for the proton transfer was taken into account with the boundary conditions N-H1-C4 = 180° and N-C4-O1 = 90°. Several initial geometries with different fixed N–C4 distances were chosen, and the energies along the paths for the proton transfer were calculated with the AM1 method and the program package VAMP 5.0.[34] An N–C4 distance of 3.5 Å proved to be suitable for modeling the proton transfer. This coincides nicely with the distance used in ref. [14b]. If a smaller distance is chosen, interaction occurs between N and C4, and the proton is transferred without an energy barrier. Figure 16 depicts the energy profile for N–C4 = 3.5 Å. This minimum distance is transferred to the calculations for the proton transfer from **4**-H$^+$ to $\mathbf{8}^-$.

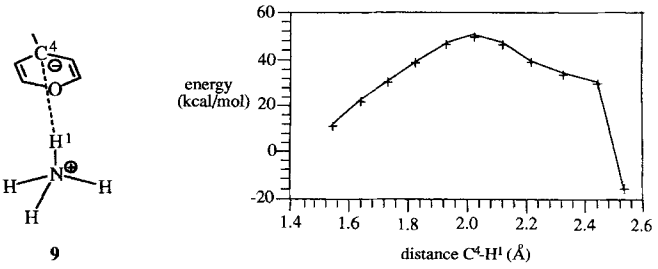

Figure 16. Calculated energies for the proton transfer in **9** with variable C4–H1 distances (N–C4 fixed at 3.5 Å).

Now 36 initial geometries are generated for the *si* protonation in the ion pair **10** (Scheme 5), which consists of **4**-H$^+$ and $\mathbf{8}^-$, whereby the dihedral C5′-N1-C4-C4a angle θ is increased in 10° steps and then kept constant during the calculation. The distance N1–C4 is kept constant at 3.5 Å. The linear transfer of the proton is maintained by the conditions N1-C4-O1 = 90° and H1-C4-O1 = 90°; all other parameters are left free for optimization. Analogous calculations were carried out for the ion pair leading to *re* protonation.

0947-6539/97/0312-2020 $ 17.50+.50/0 *Chem. Eur. J.* **1997**, *3*, No. 12

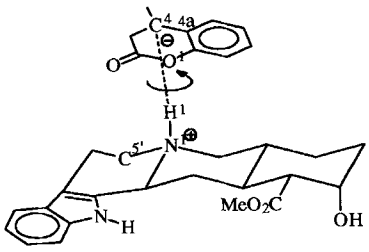

Scheme 5. The ion pair **10**, in which **4**-H^+ protonates 8^-.

For all 72 initial geometries, the reaction path for the proton transfer is calculated for H1–C4 distances between 1.8 and 2.2 Å in a step width of 0.1 Å. The 72 reaction paths obtained all have a similar shape, shown in Figure 16. They differ, however, in the energies at the summit of the reaction path. This point is always found at a H1–C4 distance of 2.0 Å.

The results are shown in Figure 17, which depicts the calculated energy of formation of the ion pairs at the highest point of the

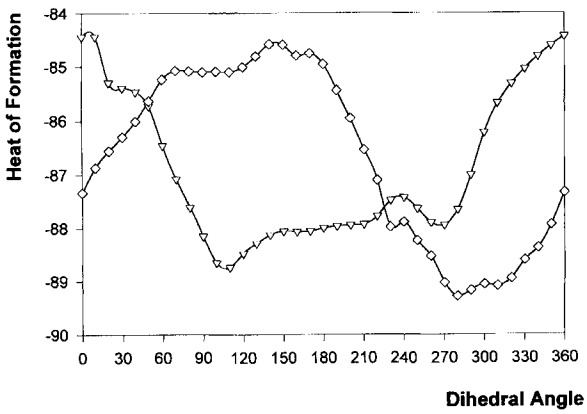

Figure 17. Transition-state energies for *re* protonation (▽) and *si* protonation (◇) in the ion pair **4**-H^+–8^- as a function of the dihedral angle C5'-N1-C4-C4a.

reaction path as a function of the dihedral angle. The lowest summit energy for *re* approach is -88.76 kcal mol^{-1}, and the corresponding value for *si* approach is -89.28 kcal mol^{-1}. The geometry for the energetically most favorable *re* protonation is shown in Figure 18, and that for the corresponding *si* approach in Figure 19.

The energy difference between *re* and *si* protonation, leading to (−)-(*S*)-**2** and (+)-(*R*)-**2**, respectively, amounts to $\Delta E = -0.52$ kcal mol^{-1} in favor of (*R*)-**2**, which corresponds to the experimental results. Regarding the assumptions made in the model and the error limits of the AM1 method, the order of magnitude of the enantiomeric excess (about 40%) is well met. The calculated energies are those for the gas phase, whilst in the real system solvated ionic structures exist, which are stabilized compared to those in the gas phase. It appears reasonable, however, to assume that the ion pairs in Figure 18 and 19 experience a similar stabilization by solvation.

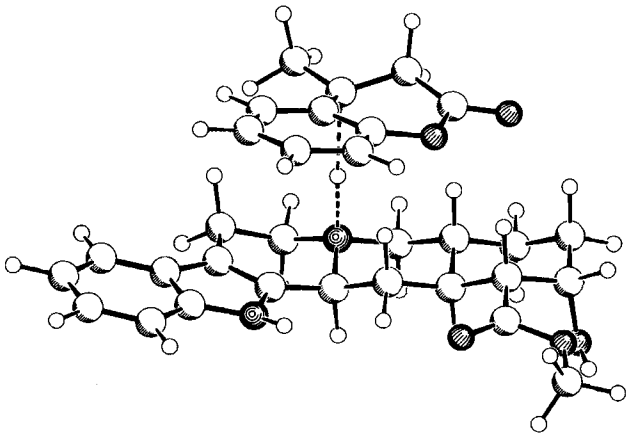

Figure 18. Geometry of the energetically most favorable *re* protonation of 8^- by **4**-H^+.

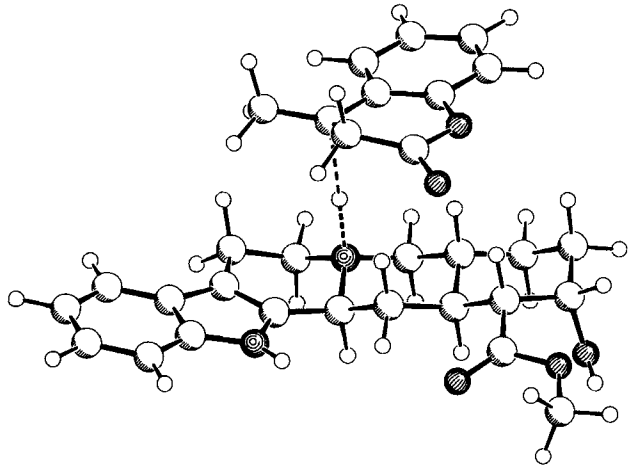

Figure 19. Geometry of the energetically most favorable *si* protonation of 8^- by **4**-H^+.

Conclusions

In acidic MeOH/H_2O (1/1) 4-methylcoumarin (**1**) is cathodically reduced to a mixture of 4-methyl-3,4-dihydrocoumarin (**2**), the hydrodimer bis-4,4'-(4-methyl-3-hydrocoumarin) (**3**), 3-(2'-hydroxyphenyl)butanoic acid (**5**) and methyl 3-(2'-hydroxyphenyl)butanoate (**6**). In the presence of yohimbine (**4**) an excess of (*R*)-**2** is obtained. Since the reduction of **1** overlaps with the proton discharge, mercury, due to its high overpotential for hydrogen evolution, is essential as cathode material for a high conversion of **1**. The chemical yields of **2** and **3** and the enantioselectivity of **2** depend on a number of reaction parameters. By combination of preparative-scale experiments and the results of electroanalytical measurements, it has been possible to propose a mechanistic model for the reaction.

The most likely mechanism under the acidic conditions of the preparative-scale experiments is that small amounts of a complex **1b** of the substrate and H_3O^+ are formed in a fast pre-equilibrium. Due to its positive charge this complex is expected to have a much more anodic reduction potential E^0(**1b**) than the loosely hydrogen-bonded 4-methylcoumarin E^0(**1a**) found under neutral conditions. The existence of a fast pre-equilibrium with a small equilibrium constant involving protons is supported by a $dE_p/d\log C^0(H^+)$ value close to 60 mV/decade. Reduc-

  0947-6539/97/0312-2021 $ 17.50+.50/0

tion of **1b** leads immediately to the formation of the neutral enol radical **7'**, whose reduction potential E^0(**7'**) is more cathodic than the reduction potential of **1** in neutral media E^0(**1a**), and **7'** is therefore not reducible at the working potential. This is supported by the fact that the reduction remains a one-electron process when the experiments are carried out in the presence of an excess of protons but in the absence of yohimbine. Therefore, the main reaction in the absence of yohimbine is the fast dimerization of the radical **7'** to form the hydrodimer **3**. The rate constant expected for the dimerization of **7'** is probably close to the rate constant for a diffusion-controlled process and at least larger than $k'_2 = 1.7 \times 10^7\ M^{-1} s^{-1}$ found for the dimerization of two hydrogen-bonded radical anions in neutral MeOH/H_2O. The yohimbineH^+ apparently catalyzes the isomerization of **7'** to the more easily reduced keto form **8'**, which is then reduced and enantioselectively protonated by yohimbineH^+. Strong support for this mechanistic suggestion comes from similar studies on the enantioselective hydrogenation of 3-methylinden-1-one.[31] An estimated value of E^0(**8'**) in the range -1.25 to -1.45 V shows that **8'**, in contrast to **7'**, will be reducible at the working potentials (-1.5 or -1.6 V) used in the preparative experiments. Since the competition is between dimerization of **7'** and yohimbine-catalyzed isomerization of **7'** to **8'**, the formation of **2** as compared to **3** will be favored by small concentrations of **1**, as found experimentally (Table 5). The much smaller amounts of **2** (with no *ee*) and larger amounts of **3** formed in the absence of yohimbine would then correspond to a much slower tautomerization in the absence of yohimbine, a mechanistic proposal which has previously been invoked for the reduction of a series of cinnamates in MeOH.[3c] Based on several observations, we also propose that yohimbineH^+ is specifically incorporated in the double layer, that is, the concentration at the location where the electron transfer takes place is higher than in the bulk. Quantum chemical calculation of the transition states for *si* and *re* protonation in the ion pair between **8**$^-$ and protonated yohimbine (**4**-H^+) show that the latter is 0.52 kcal mol^{-1} more favorable, leading to an excess of (*R*)-**2** as found experimentally.

Experimental Section

Chemicals: 4-Methylcoumarin (**1**) was prepared according to the literature procedure.[36] Yohimbine hydrochloride, Bu_4NBr, and Et_4NBr were obtained from Aldrich, and LiCl was purchased from Merck. For the electroanalytical measurements, HPLC-grade methanol and DMF from Lab-Scan and Millipore-filtered water were used.

Analytical Instrumentation: IR spectra: Bruker ISF28 spectrometer. ^1H NMR (300 MHz) and ^{13}C NMR (75.4 MHz) spectra were recorded on a Bruker WM 300 with TMS (^1H) or $CDCl_3$ (^{13}C) as internal standard. EI-GC/MS was carried out on a Varian GC1400 combined with a MAT-CH7A SS200 spectrometer. Analytical GLC was performed with an autosampler HP 5890 Series II chromatograph together with a HP 3396A integrator and a quartz capillary column (0.32 mm × 25 m, 0.52 μm, PP1). Optical yields were determined on a quartz capillary column (0.25mm × 50m, 0.52 μm, FS hydrodex β-PM) a Shimadzu GC-9A with integrator C-R 3A. HPLC was performed on a Knauer pump and UV detector (λ = 254 nm) with a reverse-phase Nucleosil 100C 18 column (diameter 8 mm) and MeOH/H_2O (1/1.3) as eluent.

Electroanalytical Measurements:

Electrodes, Cells and Instrumentation: Preliminary voltammetric measurements were carried out at room temperature on a Metrohm 663 VA Stand with an Autolab-ECOChemie PG STAT20 potentiostat controlled by the GPES 4.3 program (General Purpose Electrochemical System). The reference electrode was Ag/AgCl in EtOH/LiCl (sat). A hanging mercury drop served as working electrode and glassy carbon as counter electrode. For the kinetic measurements, the electrodes, cell and the electrochemical instrumentation, as well as the measurement and data handling procedures for derivative cyclic voltammetry and linear sweep voltammetry, were identical to those previously described.[37]

Determination of E^0: The E^0 value for **1** was determined as the midpoint between the potential of the reduction peak and the potential of the corresponding oxidation peak. Anthracene was used as an external reference in DMF, and ferrocene in MeOH and MeOH/H_2O. The E^0 value for the reference compound was determined against the same reference electrode as that used for the measurements on **1**, and $E^0 = -1.92$ V vs. SCE for anthracene[38] and $E^0 = 0.470$ V vs. SCE for ferrocene were used to convert the measured values to the SCE scale. The values given for **1** are averages of at least three sets of measurements, and the precision of the values is approximately ±3 mV in DMF and ±5 mV in MeOH and MeOH/H_2O.

Determination of Rate Constants for Dimerization: The data obtained in MeOH and MeOH/H_2O by DCV were fitted to a working curve (see Figures 5 and 8) for the rate law determined by a rate-determining radical anion–radical anion coupling, $d[\mathbf{1}^{\bullet -}]/dt = -2k[\mathbf{1}^{\bullet -}]^2$, obtained by digital simulation with the fully implicit method of Rudolph[39a] by using locally developed software.[39b] The rate constant for dimerization in DMF was determined by converting the value of $v_{0.5}$ obtained at C^0(**1**) = 0.5 mM by means of the corresponding theoretical values obtained by digital simulation. The LSV data were analyzed by Equation (*i*), as explained in the text.

Preparative Electrolyses:

Instrumentation: Current source: Bank potentiostat Model HP88. For continuous addition of **1** to the cell, a Braun motor perfusor was used. Temperature in the cell was controlled with a Colora cryothermostat MC15. The pH was measured with a Electronic Digital Greisinger pH meter GPHR 1400A and an Ingold electrode U-402.

General Procedure: **1** was added continuously during electrolysis to the cathodic compartment (charged with MeOH/H_2O/LiCl or Bu_4NBr and yohimbine hydrochloride) of a divided cell to minimize the dimerization process. *Flow cell*: 10 mL of a 0.13 M solution of **1** in MeOH/H_2O (1/1) was added over 6 h to 650 mL of electrolyte. *Beaker cell*: 6 mL of a 0.16 M solution of **1** in MeOH/H_2O (1/1) was added over 3 h to 200 mL of electrolyte. The electrolytes used were: MeOH/H_2O (1/1, 1/2, 1/4)/LiCl (0.5 M, 1.5 M) or Bu_4NBr (0.5 M). As cathode a mercury pool (38 cm^2), a glassy carbon electrode (28 cm^2) or a graphite electrode (23 cm^2) was used. The anode was platinum gauze (17 cm^2). The two compartments were separated by a glass frit (D_4) as diaphragm. A saturated calomel electrode (SCE) was used as reference electrode. After the anode and cathode compartments were charged with electrolyte the reduction of **1** was performed with stirring and the pH kept constant by dropwise addition of aqueous HCl. The pH, working potential, yohimbine concentration, working electrode, solvent composition, and the nature and concentration of electrolyte were varied (see Tables 1–6).

Isolation and Identification of Products: For work-up the methanol of the catholyte was partially removed on a rotary evaporator and 300 (flow cell) or 150 mL of distilled water (beaker cell) was added to the residue. After extraction with diethyl ether (4 × 150 mL), the combined extracts were dried ($MgSO_4$), the ether evaporated, and precipitated **3** filtered off. Toluene (20 mL) and a catalytic amount of *p*-toluenesulfonic acid monohydrate were added to the crude product to relactonize **5** and **6** into **2** by heating to reflux for 1 h at 110 °C. After toluene had been distilled off, the residue was purified by flash chromatography (diethyl ether) and the yields of **1** and **2** were determined by calibrated GLC. The optical yield of **2** was determined by GLC on a β-hydrodex column (Macherey and Nagel) at 110 °C.

The electrolyses 1, 3, 6, and 12 were performed several times to test the reproducibility of the experiments. The deviations for the yield of **1**–**3** and the *ee* of **2** were of the order of ±6% (absolute). These fluctuations are possibly due to slightly varying concentrations of **1** in experiments in which it was continuously added. The rate of addition of **1** could be kept constant in each experiment, but an equally continuous reduction was difficult to maintain due to the competing proton discharge. However, these deviations do not impair the general conclusions drawn from the tables.

0947-6539/97/0312-2022 $ 17.50+.50/0 Chem. Eur. J. 1997, 3, No. 12

4-Methyl-3,4-dihydrocoumarin (2): ref. [14a].

***meso*-4,4′-Dimethyl-4,4′-bi-3,4-dihydrocoumarin** (*meso*-**3**) was isolated by flash chromatography with toluene/EtOAc (99/1) as eluent, *meso*-**3** was more slowly eluted than *rac*-**3**. M.p. 233–235 °C; ^{1}H NMR: see ref. [14a]; ^{13}C NMR ([D$_6$]nitrobenzene): δ = 24.16 (q, CH_3, CH_3'), 38.41 (t, C3, C3′), 44.01 (s, C4, C4′), 117.12 (d, C8, C8′), 126.19 (s, C4a, C4a′), 126.46, 129.96, 130.06 (3d, C5, C5′, C6, C6′, C7, C7′), 151.96 (s, C8a, C8a′), 167.60 (s, C2, C2′); MS (GC/MS): *m*/*z* (%) 161 (100) $[M - C_{10}H_9O_2]^+$, 131 (9) $[M - C_{10}H_9O_2 - CO]^+$, 115 (20) $[C_9H_7]^+$, 105 (8), 91 (8) $[C_7H_7]^+$.

***rac*-4,4′-Dimethyl-4,4′-bi-3,4-dihydrocoumarin** (*rac*-**3**) was obtained by flash chromatography with toluene/EtOAc (99:1) as eluent. M.p. 302–303 °C; ^{1}H NMR,[14a] ^{13}C NMR ([D$_6$]nitrobenzene): δ = 23.92 (q, CH_3, CH_3'), 39.05 (t, C3, C3′), 44.02 (s, C4, C4′), 117.68 (d, C8, C8′), 125.95 (s, C4a, C4a′), 124.70, 128.62, 130.05 (3d, C5, C5′, C6, C6′, C7, C7′), 152.39 (s, C8a, C8a′), 167.74 (s, C2, C2′); MS (GC/MS): *m*/*z* (%) 161 (100) $[M - C_{10}H_9O_2]^+$, 131 (9) $[M - C_{10}H_9O_2 - CO]^+$, 115 (20) $[C_9H_7]^+$, 105 (8), 91 (8) $[C_7H_7]^+$.

X-ray crystal structure analysis of *rac*-**3**: The data set was collected with an Enraf Nonius CAD4 diffractometer. Programs used: data reduction MolEN, structure solution SHELXS-86, structure refinement SHELXL-93, graphics SCHAKAL-92. $C_{20}H_{18}O_4$, M_r = 322.34, crystal dimensions 0.20 × 0.20 × 0.10 mm, a = 14.221(1), b = 8.586(1), c = 14.088(1) Å, β = 117.66(1)°, V = 1523.6(2) Å^3, ρ_{calc} = 1.405 g cm^{-3}, μ = 7.94 cm^{-1}, empirical absorption correction by ψ-scan data ($0.946 \le C \le 0.999$), Z = 4, monoclinic, space group $C2/c$ (No. 15), λ = 1.54178 Å, T = 223 K, $\omega/2\theta$ scans, 1628 reflections collected ($-h, +k, \pm l$), $[(\sin\theta)/\lambda] = 0.62$ Å^{-1}, 1565 independent and 1186 observed reflections [$I \le 2\sigma(I)$], 110 refined parameters, R = 0.046, wR^2 = 0.123, max. residual electron density 0.22 (−0.38) e Å^{-3}, hydrogen atoms calculated and refined as riding atoms.

Crystallographic data (excluding structure factors) for the structure reported in this paper have been deposited with the Cambridge Crystallographic Data Centre as supplementary publication no. CCDC-100403. Copies of the data can be obtained free of charge on application to The Director, CCDC, 12 Union Road, Cambridge CB21EZ, UK (Fax: Int. code + (1223)336-033; e-mail: deposit@chemcrys.cam.ac.uk).

3-(2′-Hydroxyphenyl)butanoic acid (5) was isolated by preparative reverse-phase HPLC with MeOH/H_2O (1/1.3) as eluent. M.p. 113–114 °C; FT-IR (KBr): $\tilde{\nu}$ = 3453 cm^{-1} (m, OH), 1688 (s, C=O), 1222 (s, Ar–OH), 897 (m, OC–OH); ^{1}H NMR ([D$_6$]acetone): δ (J in Hz) = 1.41 (d, 3H, J = 6.9, Me), 2.66 (dd, 1H, J = 8.7, J' = 15.5, H2), 2.7 (dd, J = 6, J' = 15.5, H1), 3.65–3.8 (m, 1H, H3), 6.8–7 (m, 2H-Ar), 7.1–7.17 (m, 1H-Ar), 7.29 (dd, J = 7.6, J' = 1.7, 1H-Ar), 8.17 (s, 1H, OH), 10.3 (s, 1H, COOH); ^{13}C NMR ([D$_6$]acetone): δ = 20.8 (Me), 29.7 (C3), 41.6 (CH_2), 116.6 (C-ArH), 120.98 (C-ArH), 128.18 (C-ArH), 128.27 (C-ArH), 133.46 (C-Ar), 155.72 (C-Ar), 174.52 (C=O); MS (GLC/MS, as TMS ester): *m*/*z* (%) 324 (54) $[M]^+$, 309 (52) $[M - CH_3]^+$, 206 (70) $[M - HCOOSiMe_3]^+$, 193 (100) $[M - CH_2COOSiMe_3]^+$; Analysis: $C_{10}H_{12}O_3$ (180.2): calcd C 66.66 H 6.66; found C 66.83 H 6.52.

Methyl 3-(2′-hydroxyphenyl)butanoate (6) was isolated by flash chromatography with toluene/EtOAc (99:1) as eluent. ^{1}H NMR([D$_6$]acetone): δ (J in Hz) = 1.34 (d, 3H, J = 6.9, Me), 2.67 (s, 1H, H1), 2.69 (d, 1H, J = 1.7, H2), 3.55–3.65(m, 1H, H3), 3.65 (s, 3H, COO*Me*), 6.56 (s, 1H, OH), 6.87 (dd, 1H, J = 7.7, J' = 1.4, 1H-Ar), 6.92 (dt, 1H, J = 7.4, J' = 1.4, 1H-Ar), 7.1 (dt, 1H, J = 7.4, J' = 1.7, 1H-Ar), 7.17 (dd, 1H, J = 7.7, J' = 1.7, 1H-Ar); ^{13}C NMR ($CDCl_3$): δ = 21.03 (Me), 25.14 (C3), 42.6 (CH_2), 52.3 (COO*Me*), 117.4 (C-ArH), 121.4 (C-ArH), 127.1 (C-ArH), 128.7 (C-ArH), 132.5 (C-Ar), 153.8 (C-Ar), 175.2 (C=O); MS (GLC/MS, as TMS ester): *m*/*z* (%) = 266 (98) $[M]^+$, 251 (81) $[M - CH_3]^+$, 235 (24) $[M - OCH_3]^+$, 206 (43) $[M - HCOOCH_3]^+$, 193 (100) $[M - CH_2COOCH_3]^+$. A correct elemental analysis could not be obtained as on purification **6** was partially converted into **2.**

Quantum Chemical Calculations: See ref. [40].

Acknowledgements: Support of this research by grant ERBCHRXCT 920073 within the EU Human Capital and Mobility Programme and to B. B. by the Ministerio de Educación y Ciencia (Dirección General de Investigación Científica y Técnica) of Spain is gratefully acknowledged. M. F. N. also acknowledges the Danish Natural Science Research Council for financial support. T. L. thanks the graduate college "Hochreaktive Mehrfachbindungssysteme" of the Deutsche Forschungsgemeinschaft for support.

Received: May 5, 1997 [F 687]

[1] D. Seebach, A. R. Sting, M. Hoffmann, *Angew. Chem.* **1996**, *108*, 2880–2921; *Angew. Chem. Int. Ed. Engl.* **1996**, *35*, 2708–2745.

[2] For reviews on the earlier literature, see a) L.Eberson, L.Horner in *Organic Electrochemistry*, 1st ed. (Ed.: M. M. Baizer), Marcel Dekker, New York, **1973**, p. 869; b) J. T. Anderson, J. H. Stocker, L. Horner, in *Organic Electrochemistry*, 2nd ed. (Eds.: M. M. Baizer, H.Lund), Dekker, New York, **1983**, p. 903; c) N. L. Weinberg in *Techniques of Electroorganic Synthesis, Part 1* (Ed.: N. L. Weinberg), Wiley-Interscience, New York, **1974**, p. 254; d) W. E. Britton, in *Topics in Organic Electrochemistry* (Eds.: A. J. Fry, W. E.Britton), Plenum, New York, **1986**, p. 227; e) A. Tallec, *Bull. Soc. Chim. Fr.* **1985**, 743–761; f) T. Nonaka in *Organic Electrochemistry*, 3rd ed. (Eds.: H. Lund, M. M. Baizer), Marcel Dekker, New York, **1991**, pp. 1131–1195.

[3] a) J. H. P. Utley, M. Güllü, M. Motevalli, *J. Chem. Soc. Perkin Trans. 1* **1995**, 1961–1970; b) I. Fussing, M. Güllü, O. Hammerich, A. Hussain, M. F. Nielsen, J. H. P. Utley, *J. Chem. Soc. Perkin Trans. 2* **1996**, 649–658; c) I. Fussing, O. Hammerich, A. Hussain, M. F. Nielsen, J. H. P. Utley, *Acta Chem. Scand.*, in press.

[4] N. Kise, M. Echigo, T. Shono, *Tetrahedron Lett.* **1994**, *35*, 1897–1990.

[5] C. Zielinski, H. J. Schäfer, *Tetrahedron Lett.* **1994**, *35*, 5621–5624; C. Zielinski, Ph.D. Thesis, University of Münster, **1996**.

[6] a) B. Klotz-Berendes, H. J. Schäfer, *Angew. Chem.* **1995**, *107*, 218–220; *Angew. Chem. Int. Ed. Engl.* **1995**, *34*, 189–191; b) M. Hauck, Ph.D. Thesis, University of Münster, **1997**.

[7] R. D. Little, *Chem. Rev.* **1996**, *96*, 93–114.

[8] D. G. New, Z. Tesfai, K. D. Moeller, *J. Org. Chem.* **1996**, *61*, 1578–1598.

[9] a) D. Brown, L. Horner. *Liebigs Ann. Chem.* **1977**, 77; b) L. Horner, D. Degner. *Tetrahedron Lett.* **1968**, *56*, 5889–5892; c) L. Horner in *Organic Electrochemistry*, 2nd ed. (Eds.: H. Lund, M. M. Baizer), Dekker, New York, **1983**, pp. 945–956.

[10] a) M. Jubault, E. Raoult, D. Peltier, *Electrochim. Acta.* **1974**, *19*, 865–874; b) M. Jubault, *J. Chem. Soc. Chem. Commun.* **1980**, 953; c) M. Jubault, E. Raoult, D. Peltier. *J. Chem. Soc. Chem. Commun.* **1979**, 232–233; d) M. Jubault, E. Raoult, J. Armand, L. Boulares, *J. Chem. Soc. Chem. Commun.* **1977**, 250–251.

[11] a) A. Tallec, *Bull. Soc. Chim. Fr.* **1985**, 743–761; b) R. Hazard, S. Jaouannet, A. Tallec, *Tetrahedron* **1982**, *38*, 93–102.

[12] a) E. Kariv, H. A. Terni, E. Gileadi, *J. Electrochem. Soc.* **1973**, *120*, 639–641; b) E. Kariv, H. A. Terni, E. Gileadi, *Electrochim. Acta* **1973**, *18*, 433–441; c) E. Kariv-Miller, R. I. Pacut, G. K. Lehman, *Top. Curr. Chem.* **1988**, *148*, 99; d) K. Köster, H. Wendt, A. Lebouc, *J. Electroanal. Chem.* **1983**, *157*, 89–111; e) K. Köster, H. Wendt, A. Lebouc, *J. Electroanal. Chem.* **1982**, *138*, 209–215.

[13] a) R. N. Gourley, J. Grimshaw, P. G. Millar, *J. Chem. Soc. Chem. Comm.* **1967**, 1278–79; b) R. N. Gourley, J. Grimshaw, P. G. Millar, *J. Chem. Soc. C.* **1970**, 2318–2323; c) J. Grimshaw, P. G. Millar, *ibid.* **1970**, 2324–2325.

[14] a) N. Schoo, H. J. Schäfer, *Liebigs Ann. Chem.* **1993**, 601–607; b) U. Höweler, N. Schoo, H. J. Schäfer. *ibid.* **1993**, 609–614; c) B. Janssen, H. J. Schäfer, unpublished results.

[15] Y. Kashigawi, Y. Yanagisawa, F. Kurashima, J. Anzai, T. Osa, J. M. Bobbitt, *J. Chem. Soc. Chem. Commun.* **1996**, 2745–2746.

[16] T. Osa, Y. Kashiwagi, Y. Yanagisawa, J. Bobbit, *Chem. Commun.* **1996**, 2535–2537.

[17] K. B. Sharpless, *Chem. Rev.* **1994**, 2483–2547.

[18] S. Torii, P. Liu, N. Bhuvanesvari, C. Amatore, A. Jutand, *J. Org. Chem.* **1996**, *61*, 3055–3060.

[19] E. Steckhan, *Top. Curr. Chem.* **1987**, *142*, 1–69.

[20] The C4–C4* distance is 1.596(3) Å. This fits well into the range of C–C bond lengths between two quaternary carbon atoms of 1.566 to 1.610 Å (International Tables for Crystallography, Vol. C, Kluwer Academic Publishers, Dordrecht **1995**, p. 692).

[21] V. D. Parker in *Topics in Organic Electrochemistry* (Eds.: A. J. Fry, W. E. Britton), Plenum, New York, **1986**, ch. 2.

[22] L. Nadjo, J. M. Savéant, *J. Electroanal. Chem.* **1973**, *48*, 113.

[23] C. Reichardt, *Solvents and Solvent Effects in Organic Chemistry*, 2nd ed., VCH, Weinheim, **1990**, ch. 2 and 3.

[24] a) M. F. Nielsen, O. Hammerich, *Acta Chem. Scand.* **1987**, *B41*, 668 and references cited therein; b) the estimate is based on Equation (ii) [24c] and the

$$E_p - E^0 = -\frac{RT}{F}\left[0.783 - 0.5\left(\frac{kRT}{2F\nu}\right)\right] \quad \text{(ii)}$$

assumption that the pseudo-first-order rate constant k for the proton transfer is equal to $k_{diff} \times C^0(H^+) = 10^7$ s^{-1}; c) C. Amatore, M. Gareil, J. M. Savéant, *J. Electroanal. Chem.* **1983**, *147*, 1.

  0947-6539/97/0312-2023 $ 17.50+.50/0

[25] In the preparative work the acidity of the medium was controlled by addition of a fixed amount of HCl before the start of the electrolysis; the pH of the catholyte was monitored during the electrolysis and sufficient HCl added continuously to balance the consumption of protons by reduction and protonation. Since the substrate in most of the experiments (see Experimental Section) was added continuously during electrolysis, $C^0(\mathbf{1}) < 0.1$–0.2 mM was always maintained, and therefore $C^0(\mathrm{HCl}) = 1$ mM (pH 3) corresponds to an excess of protons relative to substrate. Since the voltammetric studies are preferentially carried out with $C^0(\mathbf{1}) \approx 1$ mM in order to achieve reasonable signal-to-noise and faradaic-to-non-faradaic current ratios, $C^0(\mathrm{HCl}) \geq 10$ mM (pH 2) was necessary to obtain a comparable excess of protons (pseudo-first-order conditions). The use of buffer was avoided to prevent complications due to additional salts.

[26] J. M. Savéant, F. Xu, *J. Electroanal. Chem.* **1986**, *208*, 197.

[27] a) E. Laviron, J.-C. Lucy, *Bull. Chem. Soc. Chim. Fr.* **1966**, 202; b) C. P. Andrieux, M. Grzeszczuk, J. M. Savéant, *J. Am. Chem. Soc.* **1991**, *113*, 8811.

[28] M. F. Nielsen, S. Spriggs, J. H. P. Utley, G. Yaping, *J. Chem. Soc. Chem. Commun.* **1994**, 1395.

[29] R. L. Munier, P. Le Xuan, A. M. Drapier, S. Meunier, *Bull. Soc. Chim. Fr.* **1982**, 250–256.

[30] M. F. Nielsen, *9th EUCHEM Conference on Organic Electrochemistry*, San Felio de Guixols, Spain, **1995**.

[31] S. Rolvering, M. F. Nielsen, H. J.Schäfer, unpublished results: 3-Methyl-2-inden-1-one is reduced at a less negative potential than **1**. At pH 3 in methanol/citrate buffer and in the absence of alkaloid it is reduced at $E_p = -0.58$ V vs. Ag/AgCl to the enol radical, which is further reduced to the enol anion at $E_p = -0.85$ V. In the presence of alkaloid, the reduction peak at -0.85 V disappears, whilst the peak current of that at -0.58 V doubles. This behavior indicates that the enol radical is tautomerized by the alkaloid to the more easily reducible keto radical.

[32] M. J. S. Dewar, E. G. Zoebisch, E. F. Healy, J. J. P. Stewart, *J. Am. Chem. Soc.* **1985**, *107*, 3902–3909.

[33] R. Stewart, *The Proton: Applications to Organic Chemistry*, in *Organic Chemistry*, *Vol. 46*, Ch. 4, Academic Press, San Diego, **1985** (Ed.: H. H. Wasserman).

[34] G. Rauhut, J. Chandrasekhar, A. Alex, T. Steinke, T. Clark, VAMP 5.0, Zentrum für Computer-Chemie der Universität Erlangen-Nürnberg, **1993**.

[35] The same calculations were done for the protonations in the ion pairs **4**-H$^-$ and **7**$^-$. Dependencies of the relative energies on the dihedral angle very similar to those in Figure 18 were obtained. The energetically most favorable transition state for *re* protonation had a relative energy of -75.07 kcal mol^{-1} and that of *si* protonation, -75.84 kcal mol^{-1}. The energy difference of about 14 kcal mol^{-1} between the two transition states for the protonation of **7**$^-$ and **8**$^-$ reflects the different energies of these two tautomeric species.

[36] a) F. Peters, H. Simonis, *Ber. Dtsch. Chem. Ges.* **1908**, *41*, 830–837; b) H. Pechman, C. Duisberg, *ibid.* **1883**, *16*, 2119–2228.

[37] a) M. F. Nielsen, S. A. Laursen, O. Hammerich, *Acta Chem. Scand.* **1990**, *44*, 932; b) M. F. Nielsen, O. Hammerich, V. D. Parker, *ibid.* **1986**, *B40*, 101.

[38] A. J. Bard, L. R. Faulkner, *Electrochemical Methods, Fundamentals and Applications*, Wiley, New York, **1980**.

[39] a) M. Rudolph, *J. Electroanal. Chem.*, **1991**, *314*, 13; b) M. L. Andersen, M. F. Nielsen, O. Hammerich, *Acta Chem. Scand.* **1995**, *49*, 503.

[40] Details of the quantum chemical calculations (MOPAC and VAMP archive entries) are available from E.-U. Würthwein upon request.

0947-6539/97/0312-2024 $ 17.50+.50/0